

## The Influence of Compressive Stress on the Order Parameter of 18R Martensites in CuAlBe Shape Memory Alloys

Ş.Nevin BALO and Mehmet CEYLAN

Firat University, Science and Arts Faculty, Department of Physics, 23169-Elazığ, Turkey  
nbalo@firat.edu.tr

(Received: 10.03.2009; Accepted: 17.04.2009)

### Abstract

Phase transformations and order parameter in the shape memory alloys are sensitive to the stress applications and these stresses may cause important changes in crystallographic properties of alloys. In this study, five stage of compressive stress were applied onto two CuAlBe shape memory alloys and some morphologic and crystallographic changes were observed. The order parameters,  $a/b$ , of 18R martensite were increased by increasing stress application.

Key Words: Compressive Stress, X-ray diffraction, Order parameter.

### CuAlBe Şekil Hatırlamalı Alaşımlardaki 18R Martensitlerin Düzen Parametresine Sıkıştırma Zorunun Etkisi

### Özet

Şekil hatırlamalı alaşımlarda faz dönüşümleri ve düzen parametresi zor uygulamalarına hassastır ve bu zorlar alaşımların kristalografik özelliklerinde önemli değişimlere sebep olabilir. Bu çalışmada beş aşamalı sıkıştırma zoru iki CuAlBe alaşımına uygulandı ve bazı morfolojik ve kristalografik değişimler gözlemlendi. 18R martensitinin düzen parametresi,  $a/b$ , artan zor uygulamasıyla artmıştır.

Anahtar Kelimeler: Sıkıştırma zoru, X-ışını difraksiyonu, Düzen Parametresi

### 1. Introduction

Martensitic transformations occurred in some metal and alloys proceed by diffusionless movements of atoms actived by temperature decreasing or by application of stress [1]. The interesting ability of Cu- based shape memory alloys to perform continuous sensing and actuating functions is due to the martensitic transformations which is thermoelastic. It is well known that the mechanism of pseudoelastic deformation in Cu-based shape memory alloy is a stress-induced martensitic transformation. Applying an external stress in appropriate temperature range can lead to the formation of martensite. This stress-induced martensite is removed when the stress is released; on complete unloading there is no residual strain.

The behaviour of material mentioned above is said to be pseudoelasticity [2].

The stress-induced martensitic transformation depends strongly on the temperature and the crystal orientation. In Cu-based shape memory alloys displayed thermoelastic martensitic transformation 24 possible martensite variants, which have the same crystalline structure but with different orientations, can form [3,4,5]. In addition, the characteristics of shape memory alloys can be modified by ageing, in particular, for a range of compositions there is a change from  $\beta$ [the parent (austenite) phase]  $\rightarrow$   $\beta'$ (18R) transformation to the  $\beta \rightarrow \gamma'$  (2H) one by ageing in parent phase [6].

Stress induced martensitic transformations in CuAlNi alloys under tensile stresses have been widely studied. A few works have been done on the stress-induced transformation under a compressive stress for Cu-Al-Ni alloys but haven't been done for CuAlBe alloys [6]. In this study, the stress-induced martensitic transformation in two CuAlBe alloys were occurred by applying five stage compressive stress on them and the affects of stress level onto order parameter of 18R martensite were determined.

## 2. Experimental Procedure

Two shape memory CuAlBe alloys were supplied by the TREFIMETAUX Company in France as polycrystalline rods (diameter 5.8 mm). These alloys were labelled Alloy1 and Alloy2; Alloy1 with a nominal composition of Cu-11.8wt%Al- 0.47wt%Be and Cu-11.6wt%Al-0.42wt%Be. All specimens obtained from Alloy1 and Alloy2 were annealed at 650°C for 15 min in the  $\beta$  phase region and cooled in boiling water (97°C) for 5 min, and then cooled again in water at room temperature and the following measurements were taken.

a) Stress Measurements: All specimens of Alloy1 and Alloy2 steeply quenched at room temperature after heat treatment before compressive stress applications. On the other specimens of Alloy1, the different compressive stress levels were applied as; 56.8, 75.7, 94.7, 113.6 and 125.7 kp mm<sup>-2</sup> with the compressing speed of 5mm min<sup>-1</sup>, at room temperature. The cracking stress value of Alloy1 was measured as 125.7 kp mm<sup>-2</sup>. On the other specimens of Alloy2, the different compressive stress levels were applied as 56.8, 75.7, 94.7, 113.6 and 118.9 kp mm<sup>-2</sup> with the same compressing speeds, at room temperature. The cracking stress value of Alloy2 was measured as 118.9 kp mm<sup>-2</sup>. These different compressive stress applications performed by using a (WPM) Industriewerk Roustein machine.

b) XRD Measurements: The X-ray piece diffractograms were taken from all of samples used as heat treated and compressive stress applied specimens by using Philips Diffractometer instrument (PW-1352) filtered Co-K $\alpha$  radiation at scanning rate of 1°/min.

c) Metallographic Observation: For optical microscopy, the specimens were polished using conventional procedures and etched in a solution composed of (5g Fe<sub>3</sub>Cl-95ml Ethanol-2ml HCl). These specimens were examined in a PME OLYMPUS optical microscope.

## 3. Results and Discussion

Alloy1 from two shape memory CuAlBe alloys investigated in this study is austenitic and Alloy2 is fully martensitic at room temperature. Transformation treatments A<sub>s</sub> (austenite starting temperature), A<sub>f</sub> (austenite finish temperature), M<sub>s</sub> (martensite starting temperature) and M<sub>f</sub> (martensite finish temperature) of these alloys were determined by DSC curves. The transformation curves of alloys are given in Figure 1 and Figure 2. The transformation temperatures are given in Table 1.

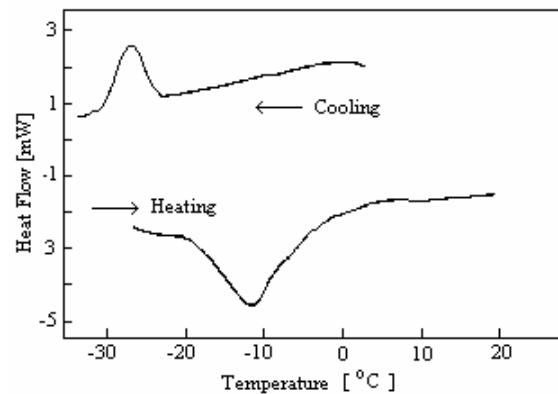


Figure 1. DSC curves of heat treated Alloy1.

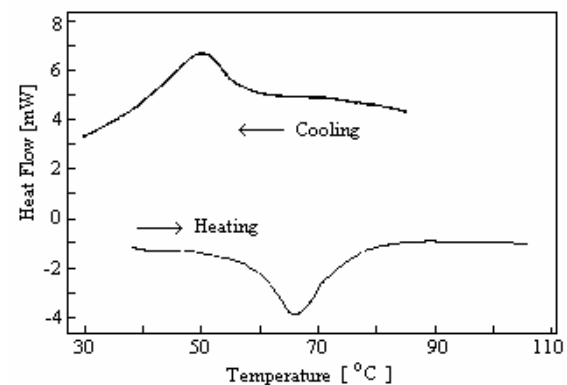
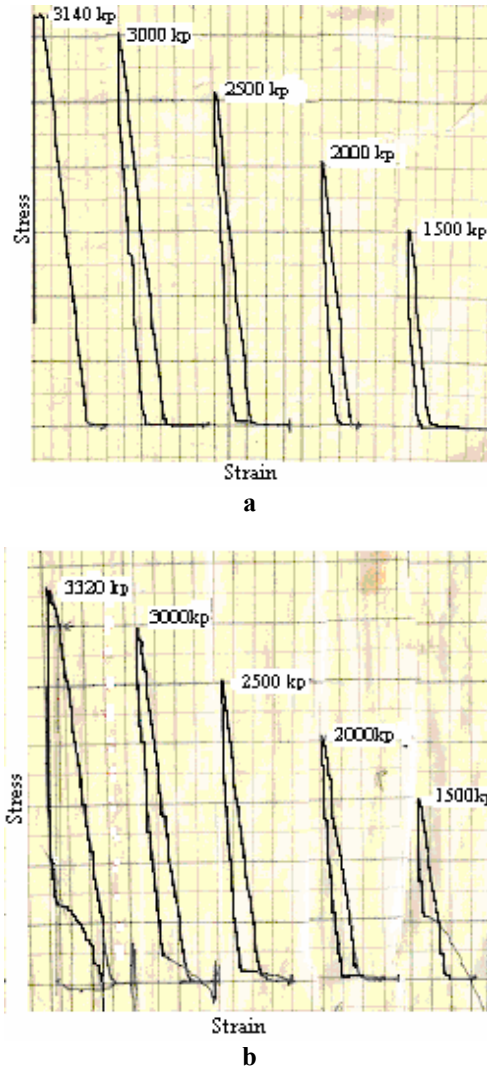


Figure 2. DSC curves of heat treated Alloy2.

**Table 1.** The transformation temperatures obtained from DSC curves

|         | A <sub>s</sub> (°C) | A <sub>f</sub> (°C) | M <sub>s</sub> (°C) | M <sub>f</sub> (°C) |
|---------|---------------------|---------------------|---------------------|---------------------|
| Alloy 1 | -18.7               | -1.6                | -23.2               | -30.4               |
| Alloy 2 | 59.6                | 77.2                | 55.3                | 41.8                |



**Figure 3.** The stress-strain curves of Alloy1 and Alloy2, respectively.

Compressing stress was applied at the temperatures above A<sub>f</sub> for specimens of Alloy1 and under M<sub>s</sub> for specimens of Alloy2. Specimens of the both alloy weren't displayed elasticity behaviour as seen from Figure 3. It can be seen from these curves that residual stress was occurred. Stress-strain curves of Alloy1 and

Alloy2 are shown in Figure 3(a and b). These compressive stress applications on these alloys were performed at room temperature.

The X-ray diffraction peaks of Alloy1 shown in Figure 4(a-f). The diffractogram taken from heat treated noncompressed sample of Alloy 1 was indexed. The sharpened peak of Alloy1 belongs to DO<sub>3</sub> structure and the other weaker peaks belong to 18R structure that developed during the cutting of this piece from the main sample. In the other diffractograms, the numbers and intensities of the diffraction peaks arising from the martensite structure increase with increasing compressive stress [7, 8].

The X-ray diffraction peaks of Alloy2 were shown in Figure 5(a-f). Heat treated noncompressed sample of Alloy2 has 18R structure. Heat treated specimens exhibit superlattice reflections. According to the changes in the positions and sharpness (intensities) of the peaks, the applied compressive stress has changed the microstructure of 18R martensite in the Alloy2 [7]. X-ray diffractograms of the compressive stressed of the alloys have been indexed on the modified ortorombic 18R unit cell and lattice parameters of the alloys were calculated by following relation [9]:

$$\frac{1}{d^2} = \frac{1}{a^2} \left( \frac{h^2}{\sin^2\beta} \right) + \frac{k^2}{b^2} + \frac{1}{c^2} \left( \frac{l^2}{\sin^2\beta} \right) - \frac{2hl\cos\beta}{ac\sin^2\beta}$$

The variations of **a/b** ratios with stress at room temperature for both alloys after step quenching and annealing have been given in Table 2 and Table 3, respectively. The martensite phase in Cu-based β-phase alloys is based on one of the {110}<sub>β</sub> basal planes. In the case where the constituent atoms are randomly distributed in the basal plane, the a/b ratio of the lattice parameters should be equal to  $\sqrt{3}/2$  while the value of this ratio is less than  $\sqrt{3}/2$  in the ordered case due to the atomic sizes of the constituent atoms for 18R martensite [10,11,12,13]. The lattice parameter of heat treated Alloy 1 specimen for cubic face centred austenite is a=5.77Å. The lattice parameters and **a/b** ratio of other heat treated Alloy1 specimens compressed until 94.7 kp mm<sup>-2</sup> stress, is given in Table 2. These **a/b** ratios is

smaller than  $\sqrt{3}/2$  as seen from Table 2. For the compressing under 113.6 and 125.7  $\text{kp mm}^{-2}$  stress of Alloy1 specimens the **a/b** ratio is bigger than  $\sqrt{3}/2$  and smaller than  $\sqrt{3}$ . **a/b** ratio of the heat treated and the compressed specimens of Alloy2 is given in Table 3. **a/b** ratios increased depending on applied stress level. **a/b** ratio at heat treated specimens is smaller than  $\sqrt{3}/2$ . The **a/b** ratio of samples, which was applied 56.8 and 75.7  $\text{kp mm}^{-2}$  compressing stress, is equal to  $\sqrt{3}/2$ . And it is bigger than  $\sqrt{3}/2$  under the other applied compressing stress. 18R structure is decomposed at stresses above 75.7  $\text{kp mm}^{-2}$ . The variations of **a/b** ratios with stress at room temperature have been plotted in Figure 6. According to these plots, the increasing compressive stress level, the order parameter **a/b**, of 18R martensites increased. The higher stress application was enhanced and favoured the martensitic phase transformations in the CuAlBe shape memory alloys.

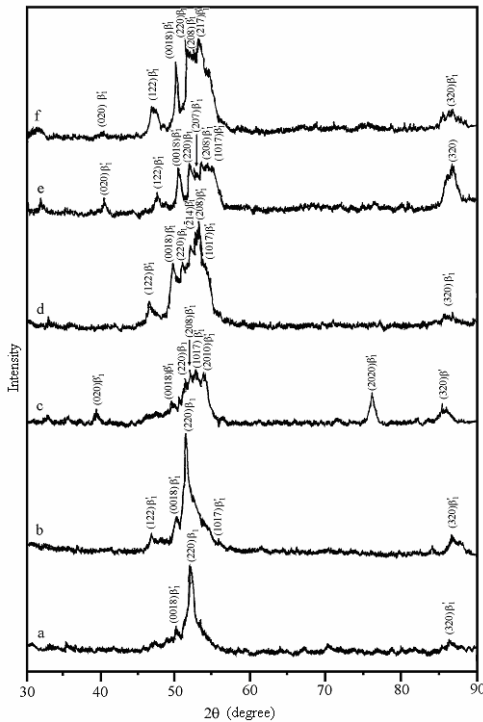


**Figure 4.** X-ray diffractograms taken from the samples of Alloy1 a) heat treated b) 56.8  $\text{kp mm}^{-2}$  c) 75.7  $\text{kp mm}^{-2}$  d) 94.7  $\text{kp mm}^{-2}$  e) 113.6  $\text{kp mm}^{-2}$  f) 125.7  $\text{kp mm}^{-2}$  [7, 8]

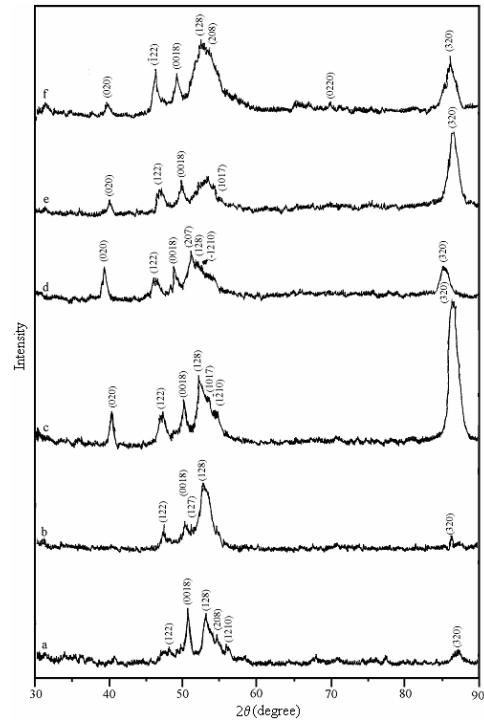


**Figure 5.** X-ray diffractograms taken from the samples of Alloy2 a) heat treated b) 56.8  $\text{kp mm}^{-2}$  c) 75.7  $\text{kp mm}^{-2}$  d) 94.7  $\text{kp mm}^{-2}$  e) 113.6  $\text{kp mm}^{-2}$  [7].

**Table 2.** The lattice parameters and a/b ratios of Alloy1

| Stress<br>( $\text{kp mm}^{-2}$ ) | DO <sub>3</sub> |       |       |       |               | 18R         |  |
|-----------------------------------|-----------------|-------|-------|-------|---------------|-------------|--|
|                                   | a (Å)           | a (Å) | b (Å) | c (Å) | $\beta^\circ$ | a/b         |  |
| -                                 | 5.77            | -     | -     | -     | -             | -           |  |
| 56.8                              | 5.87            | 4.46  | 5.32  | 38.24 | 88.93         | <b>0.83</b> |  |
| 75.7                              | 5.82            | 4.51  | 5.28  | 38.20 | 89.09         | <b>0.85</b> |  |
| 94.7                              | 5.9             | 4.45  | 5.18  | 38    | 88            | <b>0.85</b> |  |
| 113.6                             | 5.76            | 4.51  | 5.18  | 37.76 | 85.98         | <b>0.87</b> |  |
| 125.7                             | 5.77            | 4.56  | 5.16  | 37.83 | 86.06         | <b>0.88</b> |  |

**Table 3.** The lattice parameters and a/b ratios of Alloy2

| Stress<br>( $\text{kp mm}^{-2}$ ) | 18R   |       |       |               | a/b         |
|-----------------------------------|-------|-------|-------|---------------|-------------|
|                                   | a (Å) | b (Å) | c (Å) | $\beta^\circ$ |             |
| -                                 | 4.48  | 5.28  | 38.04 | 86.03         | <b>0.84</b> |
| 56.8                              | 4.50  | 5.19  | 37.89 | 88.40         | <b>0.86</b> |
| 75.7                              | 4.49  | 5.21  | 38.10 | 88.98         | <b>0.86</b> |
| 94.7                              | 4.53  | 5.16  | 38.72 | 87.30         | <b>0.87</b> |
| 113.6                             | 4.49  | 5.16  | 37.89 | 85.21         | <b>0.87</b> |
| 118.9                             | 4.56  | 5.23  | 38.47 | 86.07         | <b>0.87</b> |

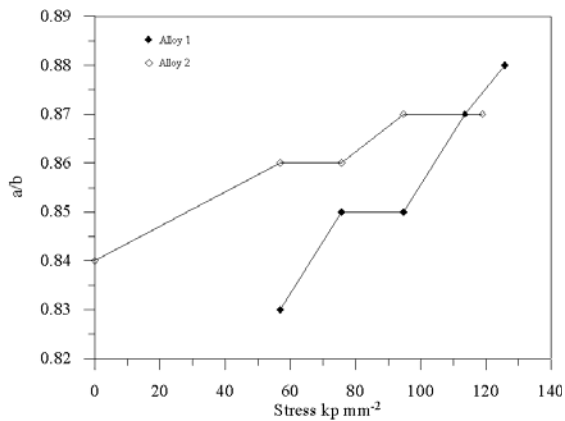


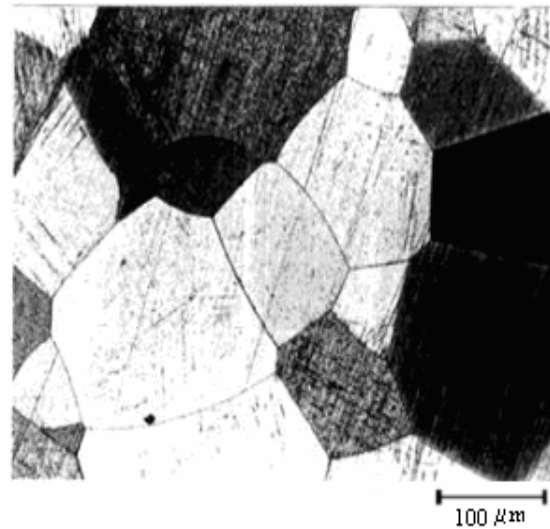
**Figure 6.** The variations of a/b values of Alloy1 and Alloy2 samples against the stress at room temperature

Optical micrographs taken from heat treated samples of both alloys are shown in Figure 7(a and b). As seen from Figure 7a the micrograph of Alloy1 includes different adjacent grains in the austenite structure. The contrast difference of these grains originates from the difference of the grain orientations [2, 7]. The micrograph of Alloy2 includes grains and martensite plates as seen from Figure 7b [7, 12].

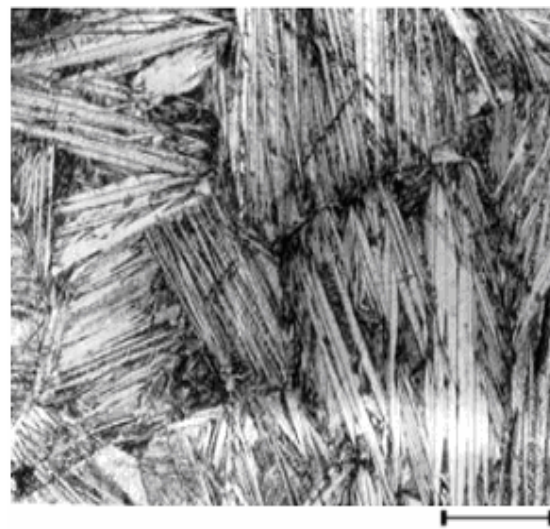
Optical micrographs taken from samples of both alloys applied 56.8 kp mm<sup>-2</sup> compressing stress are shown in Figure 8(a and b). As seen in Figure 8a, the formation of martensite plates in some grain starts when 56.8 kp mm<sup>-2</sup> compressing stress was applied to Alloy1, which it was in austenite phase at room temperature. Images of large zigzag typed martensite plates corresponding to different variants are seen in Figure 8b. This picture taken from the sample of Alloy2 after the 56.8 kp mm<sup>-2</sup> compressing stress application.

Figure 9.a is taken from the sample of Alloy1 after the 94.7 kp mm<sup>-2</sup> compressing stress application. Some twinned martensite regions labelled as (T) on the left side of picture are seen. The deformed martensite plates are also seen in the different grains. Figure 9.b is taken from the sample of Alloy2 after the 94.7 kp mm<sup>-2</sup> compressing stress application. The martensite plates become large and change into the lath martensite as seen in the left side of picture labelled as (L).

Some precipitation labelled (P) are also occurred in middle grain. The increasing of stress level was increased the amount of martensite and precipitations depending on the deformation [7, 12].

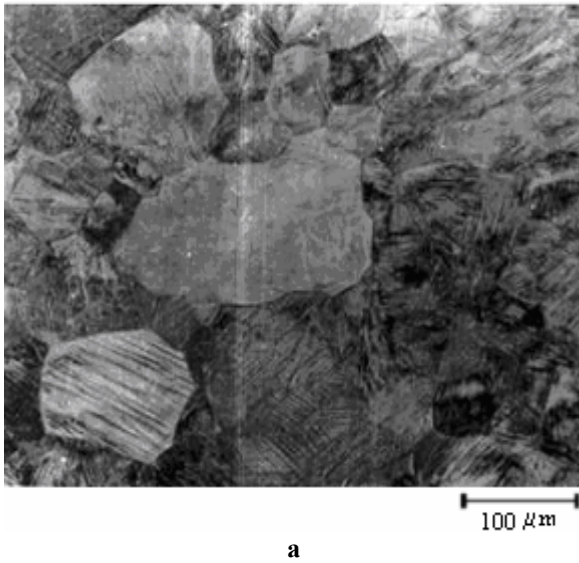


**a**

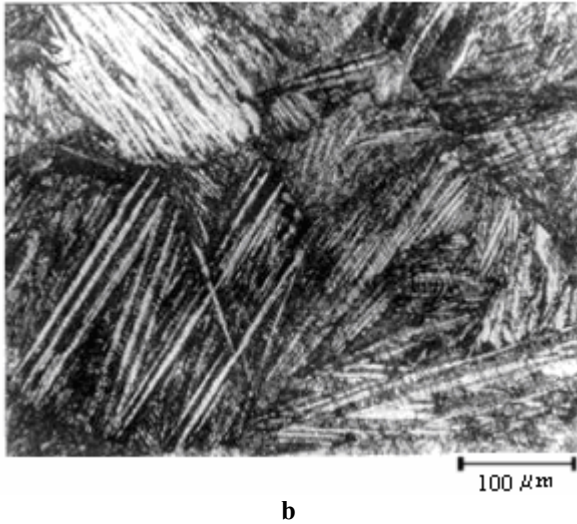


**b**

**Figure 7.** Optical micrographs of heat treated noncompressed Alloy1 and Alloy2, respectively.

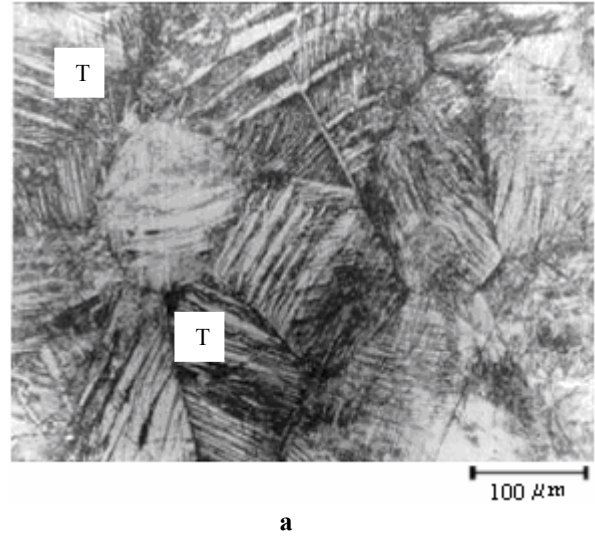


a

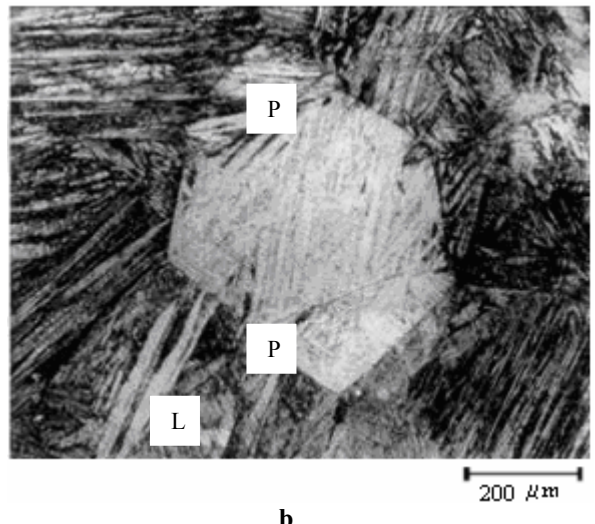


b

**Figure 8.** Optical micrographs of Alloy 1 and Alloy2 applied  $56.8 \text{ kp mm}^{-2}$  compressing stress, respectively.



a



b

**Figure 9.** Optical micrographs of Alloy 1 and Alloy2 applied  $94.7 \text{ kp mm}^{-2}$  compressing stress, respectively.

#### 4. Conclusion

It can be concluded from the above result that **a/b** ratios of Alloy1 and Alloy2 increased with the increasing of compressing stress.

Stress-induced martensites become dominant for Alloy1 with the increasing compressing stress application. At zero stress, Alloy2 is already martensite state.

#### References

1. Kennon, N.F., Dunne, D.P. (1982). Shape Strains Associated with Thermally-Induced and Stress-Induced Martensite in a Cu-Al-Ni Shape Memory Alloy. *Acta Metall.* Vol.30 429-435
2. Kaouache, B., Berveiller, S., Inal, K. Eberhardt, A., Patoor, E. (2004). Stress analysis of martensitic transformation in Cu-Al-Be polycrystalline and single-crystalline shape

- memory alloy. *Materials Science and Engineering A* 378 232–237
- Saburi, T., Wayman, C.M. (1979). Crystallographic Similarities in Shape Memory Martensites. *Acta Metall.*, 27 979-995.
  - Saburi, T., Wayman, C.M., Takata, K., Nenno, S. (1980). Shape Memory Mechanism in 18R Martensitic Alloys. *Acta Metall.*, 28 15-32.
  - Horikawa, H., Ichinose, S., Morii, K., Myazaki, S., Otsuka, K. (1988). Orientation dependence of  $\beta_1 \rightarrow \beta_1'$  stress-induced martensitic transformation in a Cu-Al-Ni alloy *Metall. Trans. A* 19 915-923.
  - Picornell C., Pons, J., Cesari, E. (2001). Stabilisation of martensite by applying compressive stress in Cu-Al-Ni single crystals. *Acta Metall.* 49 4221–4230.
  - Balo, Ş.N. (1999). The Investigation Shape Memory Properties of Cu-Al-Be and Cu-Al-Ni Alloys by Mechanical Effects Ph-D Thesis, Firat University, Institute of Science, Physics Department, Elazığ-Turkey (in Turkish) 138.
  - Balo, Ş.N., Ceylan, M., Aksoy, M. (2001). Effects of deformation the microstructure of a Cu-Al-Be shape memory alloy. *Materials Science and Engineering A* 311 151–156
  - Beeston, B.E.P., Horne, R.W., Markham R. (1972). *Electron Diffraction and Optical Diffraction Techniques* (Eds. A.M. Glauert), Cambridge, New York.
  - Adıgüzel O. (1995). Martensite ordering and stabilization in copper based shape memory alloys. *Materials Research Bulletin* 30, 755-760
  - Xuan, Q., Bohong, J., Hsu, T.Y. (1987). The Effect of Martensite Ordering on Shape Memory Effect in a Copper-Zinc-Aluminium Alloy. *Materials Science and Engineering*. 93 205–211
  - Aydoğdu, A., Aydoğdu Y., Adıgüzel, O. (1997). Improvement of Hardness and Microstructures by Ageing in Shape Memory CuAlNi Alloys. *J.Phys.IV France C5* 311-316
  - Eskil, M., Kayali, N. (2006). X-ray analysis of some shape memory CuZnAl alloys due to the cooling rate effect. *Materials Letters* 60 630-634